Membership and Multiplicity among Very Low-Mass Stars and Brown Dwarfs in the Pleiades Cluster

E. L. Martín

Division of Geological and Planetary Sciences, California Institute of Technology 150-21,
Pasadena, CA 91125, USA, ege@gps.caltech.edu

Astronomy Department, University of California at Berkeley, 601 Campbell Hall, Berkeley,
CA 94720, USA

W. Brandner

Institute for Astronomy, University of Hawaii, 2680 Woodlawn Drive, Honolulu, HI 96822,
USA, brandner@nic.ifa.hawaii.edu

J. Bouvier

Observatoire de Grenoble, B.P.53, F-38041 Grenoble Cedex 9, France,
Jerome.Bouvier@obs.ujf-grenoble.fr

K. L. Luhman & J. Stauffer

Smithsonian Astrophysical Observatory, 60 Garden St., Cambridge, MA 02138, USA,
kluhman@jayhawk.harvard.edu, stauffer@amber.harvard.edu

G. Basri

Astronomy Department, University of California at Berkeley, 601 Campbell Hall, Berkeley,
CA 94720, USA, basri@soleil.berkeley.edu

---

[1] Based in part on observations made with the NASA/ESA Hubble Space Telescope, obtained at the Space Telescope Science Institute, which is operated by the Association of Universities for Research in Astronomy, Inc., under NASA contract NAS 5-26555. These observations are associated with proposal ID 7952.

and

M. R. Zapatero Osorio

Instituto de Astrofísica de Canarias, 38200 La Laguna, Tenerife, Spain, mosorio@ll.iac.es

Received ______________; accepted ______________

to be published in The Astrophysical Journal

ABSTRACT

We present near-infrared photometry and optical spectroscopy of very low-mass stars and brown dwarf candidates in the Pleiades open cluster. The membership status of these objects is assessed using color-magnitude diagrams, lithium and spectral types. Eight objects out of 45 appear to be non-members. A search for companions among 34 very low-mass Pleiades members ($M \leq 0.09$ $M_\odot$) in high-spatial resolution images obtained with the Hubble Space Telescope and the adaptive optics system of the Canada-France-Hawaii telescope produced no resolved binaries with separations larger than 0.2 arcsec ($a \sim 27$ AU; $P \sim 444$ years). Nevertheless, we find evidence for a binary sequence in the color-magnitude diagrams, in agreement with the results of Steele & Jameson (1995) for higher mass stars. We apply the lithium test to two objects: CFHT-Pl-16, which lies in the cluster binary sequence but is unresolved in images obtained with the Hubble Space Telescope; and CFHT-Pl-18, which is binary with 0".33 separation (Martín et al. 1998). The first object passes the test, but the second object does not. We conclude that CFHT-Pl-16 is an Pleiades brown dwarf binary with separation <11 AU, and that CFHT-Pl-18 is a foreground system. We compare the multiplicity statistics of the Pleiades very low-mass stars and brown dwarfs with that of G and K-type main sequence stars in the solar neighborhood (Duquennoy & Mayor 1991). We find that there is some evidence for a deficiency of wide binary systems (separation >27 AU) among the Pleiades very low-mass members. We briefly discuss how this result can fit with current scenarios of brown dwarf formation. We correct the Pleiades substellar mass function for the contamination of cluster non-members found in this work. We find a contamination level of 33% among the brown dwarf candidates identified by Bouvier et al. (1998). Assuming a power law IMF across the substellar boundary, we find a slope dN/dM$\sim$M$^{-0.53}$, implying that the number of objects per mass bin is still rising but the contribution to the total mass of the cluster is declining in the brown dwarf regime.

Subject headings: surveys — binaries: general — stars: formation — stars: evolution — stars: low-mass, brown dwarfs, binaries — stars: luminosity function, mass function – open clusters and associations: individual (Pleiades)

1. Introduction

Brown dwarfs (BD) provide the opportunity of extending classical studies of stellar properties into the hitherto unexplored realm of objects with masses lower than the H-burning limit (0.075 M$_\odot$; e.g. Baraffe et al. 1998). Stars are frequently associated with other stars in multiple systems. 57% of nearby G-type dwarfs have H-burning companions (Abt & Levy 1976; Duquennoy & Mayor 1991, hereafter DM91). The multiplicity frequency seems to be lower among nearby M-type dwarfs (38%, Henry & McCarthy 1990; Fisher & Marcy 1992). This difference could be due to the smaller mass range available for the stellar secondaries of M dwarfs. On the other hand, the distribution of binary separations is similar for G- and M-type stars. It has a broad maximum from 3 to 30 Astronomical Units (AU). There is no indication that stellar binary properties depend on primary mass.

Stellar clusters are important for studying the multiplicity properties as a function of age, metallicity and mass. One of the best studied open clusters is the Pleiades. It is nearby (d=125 pc), young (120 Myr), the metallicity is close to solar, and there are more than 800 known members (see Hambly 1998 for a review). The Pleiades mass function has been studied over a broad mass range, from 4 M$_\odot$ to 0.04 M$_\odot$ (Hambly, Hawkins & Jameson 1993; Meusinger, Schilbach & Souchay 1996; Bouvier et al. 1998, hereafter B98). Cluster

BDs have been confirmed via the lithium test (Basri, Marcy & Graham 1996; Rebolo et al. 1996). Several imaging surveys have recently identified a numerous population of Pleiades BD candidates (B98; Festin 1998; Zapatero Osorio et al. 1999; Hambly et al. 1999). Follow-up observations of these objects is necessary for assessing their membership.

The search for BD binaries is interesting because of the following reasons: 1) Any fainter and cooler secondary of a BD should have even lower mass than the primary. 2) The binary frequency among BDs and the distribution of orbital periods and eccentricities is an important clue for understanding the formation of these objects. 3) BD binaries provide the opportunity to measure dynamical masses, which are necessary for calibrating evolutionary models. 4) The Pleiades substellar mass function needs to be corrected for binarity.

The paper is organized as follows: in Section 2 we present the observations and describe the data analysis. In Section 3 we search for companions and we construct color magnitude diagrams. In Section 4 we discuss the cluster membership of our objects, we derive parameters for the likely members, we estimate the binary frequency, and we discuss the implications of our results for the substellar mass function.

2. Observations and Data Analysis

2.1. Sample Selection

Our list was selected among the following Pleiades VLM candidate members ($M \leq 0.1\ M_{\odot}$): 'Calar' and 'Teide' objects from Zapatero Osorio et al. (1997b) and Martín et al. (1998b); 'CFHT-Pl' objects from B98; 'HHJ' objects from Hambly et al. (1993); 'MHO' objects from Stauffer et al. (1998b); 'PPl' objects from Stauffer et al. (1989, 1994) and 'Roque' objects from Zapatero Osorio et al. (1997a, 1997c, 1999). These surveys include most of the known Pleiades BD candidates.

For the HST/NICMOS program, we gave preference to objects with known near-infrared (NIR) magnitudes and/or spectral types, and we included all the Pleiades BDs with lithium detections (Rebolo et al. 1996; Martín et al. 1998; Stauffer et al. 1998a), with the exception of PPl 15 (Stauffer et al. 1994; Basri et al. 1996) because archive HST observations were already available. We observed a total of 30 objects, but one of them was a repetition (PPl1=Roque15).

For the ground-based near-IR and spectroscopic observations, we selected all the CFHT objects that had not been observed in previous campaigns. We obtained near-IR photometry for 22 objects and spectroscopy for 17.

2.2. NICMOS Observations

The targets were centered in the field of view of the NICMOS camera 1 (NIC1). Exposures of 447.95 s, 383.95 s and 383.95 s were obtained in multiple-accumulate mode with filters F110M, F145M, and F165M (Thompson et al. 1998), respectively. Each target was observed during one orbit (average visibility 52 minutes).

We used the IRAF/DIGIPHOT package for data reduction and analysis. Magnitudes for all the targets were computed based on the header keyword PHOTFNU and are given in Table 1. These values should be used with caution because the values for PHOTFNU are valid for sources with a constant flux per unit wavelength across the band pass, which might not be the case for our sources. Other limiting factors in the accuracy of the magnitudes are that we used model point spread functions (PSF) for fitting the data that did not always provide a perfect match to the observed PSF, and uncertainties in the NICMOS darks and resulting spatial variations in the background. We used on-orbits darks (as opposed to the model darks used in the standard NICMOS pipeline) to improve the photometric accuracy, but the correction was still not perfect.

2.3. Archive HST Data

The following Pleiades VLM objects have been observed with WFPC2 in other HST programs: HHJ 3, HHJ 5, HHJ 6, HHJ 10, HHJ 11, HHJ 14, HHJ 19, HHJ 36 and PPl 15. We retrieved the data from the HST archive. None of them shows any companion in the F785LP filter up to 4 magnitudes fainter than the primary at separations between 0".15 and 4."0.

2.4. Ground-based Infrared Observations

Near-IR broad-band data was collected in the following observing runs: 1) On 21-23 September 1997 at the 1 m Nickel telescope of Lick Observatory using the LIRC II camera. The wide field of view (FOV) was selected (7.29 arc mins^2, 1.71 arc secs pix^{-1}). 2) On 14-16 November 1997 using the 1.2m telescope and the STELIRCAM IR camera. STELIRCAM obtains J and K band data simultaneously using two 256x256 InSb detector arrays and a dichroic filter. The pixel scale used for these observations was 0.3 arcseconds per pixel. The typical total integration time per object was about 20 minutes, and the seeing was about 1.5 arcseconds on average. 3) On 13-15 January 1998 at the 3.6 m Canada-France-Hawaii telescope (CFHT) using the adaptive optics (AO) system PUEO (Rigaut et al. 1998) and the KIR (Doyon et al. 1998) IR camera with a 30 arcsec FOV. Integration times ranged from 100 to 150 seconds in JHK broad-band filters. Images were dark and flat-field corrected and aperture photometry performed with IRAF/APPHOT. UKIRT faint standards were observed every night for photometric calibration. For 10 of the 12 CFHT candidates observed during this run (see table 2), the adaptive optics system provided an angular resolution of 0.2 to 0.3 arcsec FWHM. The 2 remaining objects, CFHT-17 and 18, had no proper AO guiding star and have 0.4-0.5 arcsec FWHM on the final images.

2.5. Spectroscopy

We obtained spectra using the Keck II telescope with the Low Resolution Imaging Spectrograph (LRIS; Oke et al. 1995), the 4 m telescope at Kitt Peak National Observatory (KPNO) with the Cryogenic Camera (Cryocam) spectrograph, and the 4.2 m William Herschel Telescope (WHT) with ISIS. The observing log is given in Table 3. We rotated the slit in order to be at parallactic angle at the beginning of the exposure in order to minimize refraction losses.

All the CCD frames were bias subtracted, flat fielded, sky subtracted, and variance extracted using routines within IRAF[2]. We calibrated in wavelength using the emission spectrum of HgNeAr lamps. Correction for instrumental response was made using spectra obtained in the same night of flux standards with fluxes available in the IRAF environment. We did not use order-blocking filters for the Keck observations of the Pleiades BD candidates. These objects are so red that second-order contamination is negligible. We observed VB10 without filter and with the OG570 order-blocking filter. We did not find any significant contamination due to second-order light. We calibrated the LRIS spectra with the flux standard star BD+262606, which was observed the same night as the Pleiades BD candidates and with same instrumental configuration. The spectrum of the standard star obtained without filter was used blueward of 680 nm, and that obtained with the

---

[2] IRAF is distributed by National Optical Astronomy Observatory, which is operated by the Association of Universities for Research in Astronomy, Inc., under contract with the National Science Foundation.

OG570 filter was used redward of 680 nm. At KPNO we used the OG550 filter to block second-order light. The Cryocam and WHT spectra were flux calibrated with standard stars that have data available in the IRAF database.

3. Results

3.1. NICMOS Color-Magnitude Diagram

Fig. 1 shows a color-magnitude diagram (CMD hereafter) in the NICMOS F110M and F165M filters. The F145M filter is strongly affected by water vapour in the spectrum of very cool objects. The comparison with the theoretical models is less reliable because of uncertainties in the steam line lists and opacities. Our objects are plotted in the CMD together with the theoretical isochrones (age 120 Myr) of Chabrier et al. (2000). The solid line denotes the dust-free models (Nextgen; Allard et al. 1997; Hauschildt et al. 1999). The dashed line represents the new models that include dust effects (Dusty; Allard et al. 1998). It is expected that for temperatures cooler than 2800 K dust forms in the atmosphere of ultracool dwarfs (Jomes & Tsuji 1997; Marley et al. 1999). In the Nextgen models, a $T_{\rm eff}$ of 2800 K corresponds to a mass of 0.075 $M_\odot$ and M_{F110M}=10.31. The effect of dust formation in Fig. 1 is to make the objects bluer than the Nextgen isochrone because of "backwarming" (e.g. Leggett, Allard & Hauschildt 1998). We start seeing clear evidence for a turnover to bluer colors in the Pleiades sequence at M_{F110M} ∼11.5, which corresponds to a $T_{\rm eff}$=2320 K. Hence, we find that for $T_{\rm eff}$ lower than about 2300 K, dust becomes an important opacity source in the atmospheres of Pleiades BDs. The Dusty isochrone gives a good fit to the position of our faintest object (Roque 25, SpT=L0). Intermediate models between Nextgen and Dusty are not available. They seem to be required to fit the location of Pleiades BDs between M_{F110M} ∼11.5 and M_{F110M} ∼12.

All of our targets with previously known lithium detections are located close (F110M-F165M=±0.2 mag) to the Nextgen isochrone in Fig. 1. These lithium BDs are bona-fide Pleiades members and help to define the cluste sequence. They are: CFHT-Pl 15, MHO 3, PPl 1, Roque 13, Teide 1 and Teide 2. Calar 3 has not been plotted because the photometry is very uncertain due to guiding problems.

PPl 1 was observed with NIC1 at two different epochs (1 Sep 1998 and 9 Sep 1998) because we had not realized that it is actually the same object as Roque 15 (Zapatero Osorio et al. 1997c did not notice it neither). We obtained different magnitudes for the two sets of observations (Table 1). In the second epoch the object was brighter and bluer. We have marked the variation in the location of PPl 1 in the CMD of Fig. 1. The difference is much larger in the F145M filter (8 σ) than in the other two filters, suggesting variability in the steam absorption. This could be a hint of a "weather" change in the brown dwarf. Periodic photometric variability has been observed in I-band CCD observations of two cluster VLM stars, one in αPer (Martín & Zapatero Osorio 1997) and the other in the Pleiades (Terndrup et al. 1999). The light changes in these stars are probably due to surface thermal inhomogeneities (dark spots) modulated by the rotation of the object(s). On the other hand, Bailer-Jones & Mundt (1999) have recently failed to detect photometric variability in Calar 3, Roque 11 and Teide 1. Further photometric monitoring of PPl 1 is necessary to clarify if the observed variability in NICMOS filters is due to weather or magnetic spots.

The example of PPl 1 indicates that some of the spread observed in the Pleiades sequence of Fig. 1 could be due to intrinsic variability of the objects. Other sources of scatter in the CMD are unresolved binaries and non-members of the cluster. We note two examples of each kind of object. CFHT Pl 16 is brighter and redder than the rest of the sequence. It also stands out in other diagrams that are discussed in the next sections, and was noted as a possible binary by B98. We consider it as a likely unresolved binary. CFHT Pl 22 is much bluer and fainter than the Pleiades sequence. It is likely a non-member. The membership status of our sample is discussed in detail in Section 4.1.

3.2. Broad-Band Color-Magnitude Diagram

We have combined our new broad-band near-IR photometry with data available in the literature (B98; Festin 1998; Zapatero Osorio et al. 1997a,b; Martín et al. 1998c) to produce the I vs I-K CMD shown in Fig. 2. We used the following extinction corrections for all the objects: A_I=0.06, A_K=0.01. We have compared the data with theoretical isochrones (ages=100 and 120 Myr). Dusty and Nextgen models are represented with dashed and solid lines, respectively. There is a well defined observational sequence, which is conveniently fitted by the the Nextgen isochrones down to $M_{\rm I}$=14. Our faintest object, Roque 25, is bluer than the dust-free isochrone. Its location in Fig. 3 is in good agreement with the Dusty isochrone. This is explained by the greenhouse effect of dust grains (Chabrier et al. 2000).

The objects located well above the Nextgen isochrone could be binaries with nearly identical components. One of them is PPl 15, which is known to be a short-period nearly equal-mass binary (Basri & Martín 1999). The other objects are: NOT 1, HHJ 6, CFHT-Pl 6, CFHT-Pl 12 and CFHT-Pl 16. Only the later one was included in our HST/NICMOS program. HHJ 6 was observed with HST/WFPC2, and CFHT-Pl 12 was observed with the CFHT AO system. If they are binaries, they must have angular separations smaller than 0".2 (25 AU).

The objects located well below the Nextgen isochrone for $M_{\rm I} \geq 14$ are likely non-members. They are identified with five-pointed star symbols in Fig. 2. They are CFHT-Pl

19, 20 and 22.

3.3. Spectral Type-Magnitude Diagram

We display the spectra of our faintest BD objects in Fig. 3. We derived spectral types for our targets using the calibration of the pseudocontinuum index (PC3) given by Martín et al. (1999). The results are given in Table 4. Our values are in good agreement with previous work for the objects in common. Using these spectral types and those published by Steele & Jameson (1995), Martín, Rebolo & Zapatero Osorio (1996), Cossburn et al. (1997), Zapatero Osorio et al. (1997c) and Festin (1998), we have made the diagram shown in Fig. 4. Two objects lie well outside the Pleiades sequence, one above it (CFHT-Pl 16) and one below it (CFHT-Pl 26). The first one is likely an unresolved binary, and the second one is probably a non-member.

3.4. The Lithium Test in CFHT-Pl 16 and CFHT-Pl 18

CFHT-Pl 18 is an important object because it is the only binary that we have resolved in our HST images. It lies on the cluster sequence in the CMD diagrams discussed above. Martín et al. (1998a) obtained a radial velocity consistent with cluster membership. In order to confirm its membership, we obtained additional mid-resolution spectra of CFHT-Pl 18 around the LiI resonance line at 670.8 nm for applying the lithium test for BDs (Magazzù et al. 1993). If CFHT-Pl 18 is indeed a member, both components should have preserved their initial lithium content because they are fainter than the Pleiades substellar boundary (Martín et al. 1998b; Stauffer et al. 1998a). In Fig. 5, we show the final spectrum where we do not detect the lithium feature. We put an upper limit to the LiI equivalent width of 200 mA, which is a factor of 5 lower than the equivalent width (EW) measured in

Teide 1 (Rebolo et al. 1996), and a factor 2.5 lower than the EW measured in PPl 15 (Basri et al. 1996). Thus, we are confident that CFHT-Pl 18 does not pass the lithium test. This binary system appears to be located at precisely the right distance to be confused with a Pleiades member. We do not know the distance to this system because it is not a cluster member, but we can estimate it from the spectral type (M8, Martín et al. 1998a). If it has the same absolute J-band magnitude as LHS 2397a (M8, M_J=11.13, Leggett et al. 1998), we obtain a spectroscopic parallax of 105 pc. The projected separation of the binary would then be 34.5 AU.

CFHT-Pl 16 is located more than 0.5 mag above the Pleiades sequence in all the CMDs. It could be an unresolved binary with nearly identical components. Alternatively, CFHT-Pl 16 could be a non-member. We obtained Keck/LRIS mid-resolution spectroscopy to test its membership. The reduced spectrum is shown in Fig. 5. We clearly detect H_α in emission with EW=-6.1 A. The quality of our spectrum is barely sufficient for a detection of the LiI resonance line. There is an absorption feature at the position of the LiI resonance line with EW$\sim$1.2 A, which is similar to the EW of Teide 1 (Rebolo et al. 1996), but there are also noise features of similar strength elsewhere in the spectrum. We estimate that the probability of having a noise feature at the position of the LiI line is <10%, i.e. low but not negligible. We measured a heliocentric radial velocity of 13±5 km/s using the H_α feature, which is consistent with the radial velocities of VLM Pleiades members (Martín et al. 1998b).

3.5. Search for Companions

Since the NICMOS PSF can vary significantly from one HST orbit to the next, we used all of the HST/NICMOS pointings to build up a library of HST/NIC1 PSFs in all three filters (F110M, F145M, anf F165M). For each set of observation, we then identified the best matching PSF in the library for PSF subtraction. Sub-pixel offsets between target and PSF were computed by cross-correlating the individual frames. The PSF was then Fourier-shifted, scaled, and subtracted.

Fig. 6 shows examples of NIC1 images before and after point spread function (PSF) subtraction. The dark line seen in each image is the boundary between the individual NICMOS quadrants. In the original image we can clearly see the first and second airy rings. They are considerably reduced in the subtracted image.

We have estimated limiting sensitivities to the presence of companions as a function of separation from the primary. They are given in Table 5 for two different separations. A few radial averages of the limits to the presence of companions in NICMOS images are shown in Fig. 7. They were derived under the assumption that we would detect a source if the counts in the central pixel of its PSF are at least 3 times the sigma of the background. The four objects, namely CFHT-Pl 15, CFHT-Pl 19, HHJ 2 and MHO 3, for which the residuals of the PSF subtraction were high have been flagged in Table 5. The residuals could be due to the presence of faint companions within 5 pixels (0.215") of the primary, or to unrepeatable structure in the PSF.

We have not found any distant (sep.>1") companions in the near-IR images taken at CFHT and Mt Hopkins. Any companion up to 3 magnitudes fainter than the primary in the separation range 1 to 8 arcseconds, should have been detected.

4. Membership in the Pleiades

4.1. Membership criteria

The membership criteria that we have used are the following: 1) Is the object a dwarf or a giant? All the objects for which we have low-resolution spectra have KI and NaI lines similar to those of dwarfs. Because of the low-resolution of most of our spectra, the NaI doublet at 818.3 and 819.0 nm is blended with telluric absorption and we cannot derive an accurate equivalent width. Thus, we do not use the strength of the line as a membership criterion (Martín et al. 1996). 2) Is the radial velocity similar to those of known members? We have used radial velocity data from the literature (Basri et al. 1996; Martín et al. 1998b; Stauffer et al. 1998b). 3) Is the proper motion similar to the cluster? We have used proper motion data from the literature (Hambly et al. 1993; Hambly et al. 1999). 4) Does the object have lithium? Pleiades members fainter than I∼17.8 should have lithium (Martín et al. 1998b; Stauffer et al. 1998b). Brighter objects could have lithium if they are binaries (PPl 1). 5) Does the object have H_α in emission? The majority of Pleiades members do show H_α in emission because of their young age. However, H_α is variable and sometimes not detected. For example, we did not detect it in our Keck spectrum of Teide 1, but it was previously detected by Rebolo et al. (1996). We do not reject any candidate member solely on basis of lack of H_α emission, but we note that many non-members do not have H_α emission, suggesting that they are relatively old field dwarfs. 6) We checked the position of each object in the spectral type versus apparent I-band magnitude (Fig. 4). The lithium BDs are considered as benchmark objects, and most of the BD candidates are located near them. Objects that deviate from the sequence by more than 0.8 magnitudes are considered as likely non-members. 7) The location of the lithium BDs in the I versus (I-K) and F110M versus (F110M-F165M) CMDs is well fitted with the Nextgen isochrone. On the other hand, the location of Roque 25 in the same CMDs is fitted by the Dusty isochrone. Objects that are 3σ away from the isochrones are considered as likely non-members.

We summarize our assessment of the membership status of 45 objects in Table 6. We confirm the Pleiades membership of 37 VLM stars and BDs, and reject 8 objects as non-members. The later objects are excluded from our calculation of binary statistics in the Pleiades cluster.

4.2. Physical Parameters

In order to derive the physical parameters of the objects that we consider as likely Pleiades members, we adopted a common age, distance and metallicity of 120 Myr, 125 pc and solar, respectively.

The only way to infer masses for our objects is to compare their location in the CMD with theoretical calculations. In Fig. 8, we show the theoretical mass-luminosity relationships for several near-IR filters that we have adopted. The behaviour of the NICMOS filters F110M and F165M mimics that of the *J* and *H* broad-band filters, respectively. The sensitivity to dust effects changes with λ and mass (temperature) across these plots. We have minimized the dependence of our results on the role of dust in the atmosphere by using the filters that show less sensitivity to the choice of model (Nextgen or Dusty) for a given mass. For all the objects we used the absolute magnitudes in the J and F110M filters (we averaged the two of them if both magnitudes were available) and the NEXTGEN models, but for Roque 25 we used the K-band absolute magnitude and the DUSTY model. Our mass estimates for the CFHT objects are consistent within ± 0.005 $M_\odot$ with those derived by B98 using three different sets of models and absolute I-band magnitudes.

5. Binary statistics

The masses of the primaries considered in this study range from 0.14 $M_\odot$ (CFHT-Pl-1, I=16.1, B98) to 0.035 $M_\odot$ (Roque 25, I=21.17, Martín et al. 1998c). The masses of the primaries observed with high-resolution techniques (AO and HST) are all lower than 0.11 $M_\odot$ (HHJ19, I=16.7, Hambly et al. 1993). We estimated upper limits to the masses of undetected companions using the DUSTY models and the sensitivity limits in the *K* and/or F165M filters. The average limits on the mass ratios ($q=M_2/M_1$) for different separation ranges are given in Table 7. The limits on close (<1”) companions come from the HST and AO images, and the limits on distant companions were derived from the ground-based K-band images.

Since the only binary that we found, CFHT-Pl-18, did not pass the lithium test, we have found zero resolved binaries in our sample. However, this null result does not necessarily imply that the binary frequency among Pleiades VLM members is very low. Basri & Martín (1999) found that PPl 15 is a double-lined binary with a period of only 5.8 days. Zapatero Osorio et al. (1997a) had noticed that this object lies on the binary sequence. Five other Pleiades VLM members also lie in the binary sequence in the CMD of Fig. 2. We consider them as likely binaries with nearly-identical components. Two of them (lying near HHJ 6) have not been observed with HST or AO. Three of them (HHJ 6, CFHT-Pl-12 and 16) are not resolved with HST or CFHT/AO. Steele & Jameson (1995) have suggested that 46% of Pleiades VLM stars are multiple on the basis of a spectroscopic study of temperature indicators. However, none of their HHJ candidate binaries observed with HST/WFPC were resolved.

Bouvier, Rigaut & Nadeau (1997) carried out an AO search for binaries among 144 G- and K-type Pleiades members. They found that the binary frequency and period distribution of their sample is similar to that of DM91. Since the DM91 study has better statistics, we have used their orbital period and mass ratio distributions for predicting the number of binaries expected in our sample. The results are given in the third column of Table 7. We have converted the observed upper limits on components separations on the plane of the sky (s) to semi-major axes (a) using a cluster distance of 125 pc and s/a=0.92 (Heacox & Gathright 1994). Considering our sample of Pleiades BDs observed with HST/NICMOS, we find that there is a factor of ∼3 excess of binaries with respect to the distribution of DM91 for separations smaller than 10.9 AU, which corresponds to orbital periods shorter than ∼110 years. However, because of the small size of our sample we find that the difference between the Pleiades and the field binaries is significant only at the 1 σ level. On the other hand, it is more significant that we do not find any binaries with separations larger than ∼27 AU. The lack of Pleiades VLM systems with periods longer than 444 years (3.4 expected, 0 found) is a 2 σ effect for Poisson statistics.

Reid & Gizis (1997) obtained HST observations of 53 Hyades M-type members (primary mass $\leq$0.3 $M_{\odot}$). They found nine binaries with $q>0.5$ in the separation range 14 to 825 AU, consistent with observations of M-dwarfs in the solar neighborhood. If the binary properties of our Pleiades VLM sample was similar to that of the Hyades sample of Reid & Gizis, we should have found 2 binaries with separations larger than 30 AU.

When they grow old, the Pleiades VLM stars and BDs will become cooler and will look similar to L-type field dwarfs. The first three field binaries with L-dwarf components have been recently discovered (Martín, Brandner & Basri 1999; Koerner et al. 1999). All of them have separations less than 10 AU, and would not have been resolved in our survey if they were at the Pleiades distance. There is no bias against finding wider binaries because the FOV in these searches is ≥100 AU. In fact, no wide doubles have been reported in the infrared images of ∼ 100 L dwarfs and ∼15 methane dwarfs identified so far in the DENIS, Sloan and 2MASS surveys. However, there has not been a survey for spectroscopic binaries among ultracool dwarfs. There could be many short-period VLM binaries that have not been identified yet. The null result of our survey for Pleiades BD binaries is consistent with the properties of the field BD binaries found so far.

The median orbital separation of the main-sequence stars studied by DM91 is 23 AU (Heacox 1998). Two Pleiades BD binaries (PPl 15 and CFHT Pl 16) and three field BD binaries have been identified with separations <23 AU, but no BD binaries are known to have separations ≥23 AU. The systematically small separations of the BD binaries with respect to the DM91 sample, suggest that there is a difference in population characteristics. The small numbers involved preclude any definitive conclusion in this regard, but it is worth of mention and brief discussion.

The mass of the primary could be an important factor in the the process of binary formation. Basri & Martín (1999) suggested that the formation of substellar binaries is biased toward smaller separations than the formation of stellar binaries because the probability of finding a short-period binary like PPl 15 from a normal (DM91-type) binary distribution is only ∼10%. Another interesting proposition is that of a "brown dwarf desert", i.e. a scarcity of BD secondaries to G and K dwarfs within 2 AU of the primary (Marcy & Butler 1998). It seems that BDs, as objects representative of the tail of the stellar mass function, could provide important hints about binary formation.

We briefly consider three possible scenarios that could explain a difference in the characteristics of BD binaries with respect to the DM91 sample: (1) Disruption of wide binaries due to dynamical interactions with the stellar members of the cluster. This process has been invoked by Kroupa, Petr & McCaughrean (1999) to explain the binary frequency of stars in the Trapezium cluster. An important test of this scenario is the binary frequency of hard binaries, which should be independent of primary mass. (2) If VLM stars and BDs usually come from the dynamical ejection of VLM fragments from protostellar aggregates (Laughlin & Lin, private communication), the ones that are more likely to survive are close binaries with nearly-identical component. Such an scenario has two constraints to overcome. The typical ejection velocity of the ejected VLM star or BD cannot be much larger than the escape velocity from the Pleiades cluster. The mechanism has to be extremely efficient because BDs are quite numerous. (3) Numerical simulations of molecular cloud fragmentation have shown that slower rotating cloud cores form closer binaries than when the clouds are rapidly rotating (Boss 1993). Small cloud cores that start collapse from high initial densities form even closer binaries. This scenario seems provide a natural way of explaining the absence of wide BD binaries and an excess of close systems. Furthermore, the BD desert around solar-type stars can also be explained by fragmentation processes (Bate 2000).

6. The Pleiades substellar mass function

We have presented NIR photometry and low-resolution spectroscopy for all the BD candidates reported by B98. We have also applied the lithium test to CFHT-Pl-16 and 18. The membership status of all the CFHT BD candidates is summarized in Table 6. We restrict ourselves to the CFHT sample for addressing the issue of the substellar mass function, because the level of follow-up observations of the BD candidates coming from other surveys is still incomplete.

The level of field star contamination among Pleiades BD candidates was assessed by B98 using two statistical approaches. They compared the mass of Pleiades members and field stars in the same volume, and they used a field luminosity function. Both methods were in good agreement, and suggested a contamination of 25% . We confirm the membership of 12 Pleiades CFHT BD candidates out of the 18 included in B98. The 6 non-members are all foreground cool M dwarfs. We find a contamination of 33%, which is somewhat higher than the estimate of B98. These authors obtained a power-law index in a log-log plot ($dN/dM \sim M^{\alpha}$) of α=-0.6 for the cluster IMF across the substellar boundary. We revise this slope downwards to a value of α=-0.53 , implying that the number of BDs per decreasing mass bin is moderately rising, but their relative contribution to the total mass of the Pleiades cluster is diminishing.

We cannot make a detailed correction of the IMF for the binary fraction of the CFHT

BDs because we have not resolved any system. Nevertheless, we believe that the binary corrections are probably not very important because there does not seem to be many BD companions to stars, and because our search for binaries suggest that BDs do not have a higher multiplicity frequency than M-type stars.

Acknowledgments: This research makes use of data collected at the Hubble Space Telescope, the Canada-France-Hawaii telescope, the Lick Nickel telescope and the Mt Hopkins telescope. Some of the data presented herein were obtained at the W.M. Keck Observatory, which is operated as a scientific partnership among the California Institute of Technology, the University of California and the National Aeronautics and Space Administration. The Observatory was made possible by the generous financial support of the W.M. Keck Foundation. We are grateful to the HST staff (particularly, Beth Perriello and Al Schultz) for their assistance. We thank France Allard, Isabelle Baraffe, Gilles Chabrier and Peter Hauschildt for making their evolutionary models available to us. EM thanks Alan Boss, Greg Laughlin and Doug Lin for discussions about the formation of brown dwarf binaries. GB acknowledges the support of NSF through grant AST96-18439. FA was supported by NASA through grants 110-96LTSA and NAG5-3435. Funding for this publication was provided by NASA through Proposal GO-7899 submitted to the Space Telescope Science Institute, which is operated by the Association of UNiversities for Research in Astronomy, Inc., under NASA contract NAS5-26555.

REFERENCES

Abt, H. A. & Levitt, S. G. 1976, ApJS, 30, 273 F

Allard, F., Hauschildt, P. H., Alexander, D. R. & Starrfield, S. 1997, ARAA, 35, 137

Allard, F., Alexander, D. R. & Hauschildt, P. H. 1998, ASP Conf. Ser. 154, The Tenth Cambridge Workshop on Cool Stars, Stellar Systems and the Sun, Edited by R. A. Donahue and J. A. Bookbinder, p.63

Bailer-Jones, C. A. L. & Mundt, R. 1999, A&A, 348, 800

Baraffe, I., Chabrier, G., Allard, F., & Hauschildt, P.H. 1998, A&A, 337, 403

Basri, G., Marcy, G., & Graham, J. R. 1996, ApJ, 458, 600

Basri, G., & Martín, E.L. 1999, AJ, 1727, 2460

Bate, M. 2000, MNRAS, in press

Boss, A. 1993, in "The Realm of Interacting Binary Stars", ed. J. Sahade, Kluwer Academic Publishers, p. 355

Bouvier, J., Rigaut, F. & Nadeau, D. 1997, A&A, 323, 139

Bouvier, J., Stauffer, J. R., Martín, E.L., Barrado y Navascués, D., Wallace, B. & Béjar, V.J.S. 1998, A&A, 336, 490 (B98)

Chabrier, G., Allard, F., Baraffe, I. & Hauschildt, P. 2000, A&A, submitted

Cossburn, M. R., Hodgkin, S. T., Jameson, R. F. & Pinfield, D. J. 1997, MNRAS, 288, L23

Doyon, R. et al. 1998, in: Fowler A.M. (ed.), SPIE Proc. 3354, Infrared Astronomical Instrumentation

Duquennoy, A. & Mayor, M. 1991, A&A, 248, 485

Festin, L. 1998, A&A, 333, 497

Fisher, D. A. & Marcy, G. W. 1992, ApJ, 396, 178

Reid, I. N. & Gizis, J. E. 1997, AJ, 114, 1992

Hambly, N. C. 1998, in “Brown Dwarfs and Extrasolar Planets”, eds R. Rebolo, E. L. Martín & M. R. Zapatero Osorio, ASP Conf. Series, 134, 11

Hambly, N. C., Hawkins, M. R. S., & Jameson, R. F. 1993, A&AS, 100, 607

Hambly, N. C., Hodgkin, S. T., Cossburn, M. R. & Jameson, R. F. 1999, MNRAS, 303, 835

Hauschildt, P. H., Allard, F. & Baron, E. 1999, ApJ, 512, 377

Heacox, W. D. & Gathright, J. 1994, AJ, 108, 1101

Heacox, W. D. 1998, AJ, 115, 325

Henry, T. J. & McCarthy, D. W. 1990, ApJ, 350, 334

Jones, H. R. A. & Tsuji, T. 1997, ApJ, 480, L39

Koerner, D. W., Kirkpatrick, J. D., McElwain, M. W. & Bonaventura, N. R. 1999, ApJ, 526, L25

Kroupa, P., Petr, M. G. & McCaughrean, M. J. 1999, NewA, 4, 495

Leggett, S. K., Allard, F. & Hauschildt, P. H. 1998, ApJ, 509, 836

Magazzù, A., Martín, E. L. & Rebolo, R. 1993, ApJ, 404, L17

Marcy, G. & Butler, R. P. 1998, ARA&A, 36, 57

Martín, E. L., Rebolo, R., & Zapatero Osorio, M. R. 1996, ApJ, 469, 706

Martín, E. L., Basri, G., Brandner, W., Bouvier, J., Zapatero Osorio, M. R., Rebolo, R., Stauffer, J., Allard, F., Baraffe, I. & Hodgkin, S. 1998a, ApJ, 509, L113

Martín, E. L., Basri, G., Gallegos, J. E., Rebolo, R., Zapatero Osorio, M. R. & Béjar, V. J. S. 1998b, ApJ, 499, L61

Martín, E. L., Basri, G., Zapatero Osorio, M. R., Rebolo, R., & García López, R. J. 1998c, ApJ, 507, L41

Martín, E. L. & Zapatero Osorio, M. R. 1997, MNRAS, 286, L17

Martín, E. L., Brandner, W. & Basri, G. 1999, Science, 283, 1718

Marley, M. S., Gelino, C., Stephens, D., Lunine, J. I. & Friedman, R. 1999, ApJ, 513, 879

Oke, J. B., Cohen, J. G., Carr, M. et al. 1995, PASP, 107, 375

Rebolo, R., Martín, E. L., Basri, G., Marcy, G. W., & Zapatero Osorio, M. R. 1996, ApJ, 469, L53

Rigaut, F. et al. 1998, PASP 110, 152

Stauffer, J. R., Hamilton, D., & Probst, R. 1994, AJ, 108, 155

Stauffer, J. R., Hamilton, D., Probst, R., Rieke, G. & Mateo, M. 1989, ApJ, 344, L21

Stauffer, J. R., Schultz, G. & Kirkpatrick, J.D. 1998a, ApJ, 499, L199

Stauffer, J. R., Schild, R., Barrado y Navascués, D., Backman, D. E., Angelova, A. M., Kirkpatrick, J. D., Hambly, N. & Vanzi, L. 1998b, ApJ, 504, 805

Steele, I. A. & Jameson, R. F. 1995, MNRAS, 272, 630

Terndrup, D. M., Krishnamurthi, A., Pinsonneault, M. H. & Stauffer, J. R. AJ, in press

Thompson, R.I., Rieke, M.J., Schneider, G., Hines, D. & Corbin, M.R. 1998, ApJ, 492, L95

Zapatero Osorio, M. R., Martín, E. L., & Rebolo, R. 1997a, A&A, 323, 105

Zapatero Osorio, M. R., Rebolo, R., & Martín, E. L. 1997b, A&A, 317, 164

Zapatero Osorio, M. R., Rebolo, R., Martín, E. L., Basri, G., Magazzù, A., Hodgkin, S. T., Jameson, R.F. & Cossburn, M. R. 1997c, ApJ, 491, L81

Zapatero Osorio, M. R., Rebolo, R., Martín, E. L., Hodgkin, S. T., Cossburn, M. R., Magazzù, A., Steele, I. A. & Jameson, R.F. 1999, A&AS, 134, 537

This manuscript was prepared with the AAS LaTeX macros v5.0.

Table 1. NICMOS photometry for Pleiades VLM candidates

Name	Other Name	m(F110M)	m(F145M)	m(F165M)
Calar 3*	CFHT 21	17.07±0.16	16.76±0.40	16.24±0.20
CFHT-Pl 15		16.53±0.01	15.87±0.01	15.22±0.01
CFHT-Pl 16		16.28±0.04	15.61±0.02	14.95±0.02
CFHT-Pl 17		16.76±0.05	16.03±0.01	15.43±0.01
CFHT-Pl 18 A		16.96±0.07	16.31±0.03	15.77±0.04
CFHT-Pl 18 B		17.74±0.14	17.11±0.07	16.50±0.07
CFHT-Pl 19		16.93±0.09	16.37±0.01	15.77±0.02
CFHT-Pl 20		17.17±0.05	16.40±0.09	15.90±0.02
CFHT-Pl 22		17.41±0.09	17.03±0.03	16.53±0.02
CFHT-Pl 23		17.09±0.05	16.31±0.09	15.71±0.02
CFHT-Pl 25		17.30±0.05	16.59±0.03	15.93±0.03
HHJ 2		15.85±0.04	15.19±0.01	14.75±0.01
HHJ 8		15.53±0.02	14.86±0.01	14.42±0.01
MHO 1		15.90±0.06	15.41±0.01	14.91±0.01
MHO 3		16.08±0.08	15.51±0.02	14.90±0.01
MHO 6		15.97±0.04	15.32±0.02	14.83±0.02
PIZ 1		17.11±0.11	16.53±0.13	15.79±0.05
PPl 1	Roque 15	15.97±0.01	15.48±0.01	14.73±0.01
		15.90±0.03	15.31±0.01	14.71±0.01
PPL 14		15.82±0.03	15.33±0.01	14.82±0.01
Roque 4		17.24±0.04	16.55±0.04	15.86±0.02
Roque 7	CFHT-Pl 24	17.12±0.03	16.43±0.02	15.79±0.01
Roque 11		16.65±0.03	16.00±0.02	15.43±0.02
Roque 12		16.59±0.05	15.89±0.03	15.34±0.02
Roque 13		16.27±0.01	15.67±0.01	15.04±0.01

Table 1—Continued

Name	Other Name	m(F110M)	m(F145M)	m(F165M)
Roque 14		16.11±0.05	15.50±0.07	14.87±0.04
Roque 16	CFHT-Pl 11	16.16±0.03	15.49±0.03	14.97±0.01
Roque 17		15.91±0.04	15.31±0.01	14.73±0.01
Roque 25		18.32±0.23	17.77±0.09	16.77±0.02
Teide 1		16.92±0.03	16.18±0.01	15.59±0.01
Teide 2	CFHT-Pl 13	16.18±0.04	15.48±0.01	14.97±0.01

*Trailed image because of guiding error

Note. — The error bars are 1 σ standard deviations.

Table 2. New ground-based photometry for Pleiades VLM candidates

Name	m(J)	m(H)	m(K)	Telescope
Calar 3	16.10±0.02	15.42±0.04	14.90±0.07	CFHT
CFHT-Pl 1	14.41±0.03		13.50±0.10	MHO
CFHT-Pl 2	14.69±0.03		13.71±0.10	MHO
CFHT-Pl 3	14.81±0.03		13.82±0.10	MHO
CFHT-Pl 4	14.96±0.03		14.01±0.10	MHO
CFHT-Pl 5	15.08±0.03		14.06±0.10	MHO
CFHT-Pl 6	14.89±0.03		13.78±0.10	MHO
CFHT-Pl 7	15.42±0.03		14.43±0.10	MHO
CFHT-Pl 8	15.16±0.03		14.13±0.10	MHO
CFHT-Pl 9	15.46±0.10			Lick
	15.44±0.03		14.44±0.10	MHO
CFHT-Pl 10	15.49±0.10			Lick
	15.53±0.05		14.49±0.10	MHO
CFHT-Pl 12	15.10±0.02	14.51±0.04	14.11±0.07	CFHT
	15.17±0.10			Lick
	15.23±0.03		14.14±0.10	MHO
CFHT-Pl 15	16.00±0.02	15.22±0.04	14.87±0.07	CFHT
	15.98±0.03		14.80±0.10	MHO
CFHT-Pl 16	15.65±0.02	14.85±0.04	14.39±0.07	CFHT
	15.69±0.10			Lick
CFHT-Pl 17	15.98±0.02	15.20±0.04	14.90±0.07	CFHT
	16.05±0.10			Lick
CFHT-Pl 18	15.95±0.02	15.23±0.04	14.80±0.07	CFHT
CFHT-Pl 19	16.51±0.02	15.70±0.04	15.47±0.07	CFHT
	16.48±0.10			Lick

Table 2—Continued

Name	m(J)	m(H)	m(K)	Telescope
CFHT-Pl 20	16.56±0.02	15.88±0.04	15.56±0.07	CFHT
	16.54±0.10			Lick
CFHT-Pl 22	17.11±0.02	16.61±0.03	15.95±0.10	CFHT
CFHT-Pl 23	16.46±0.02	15.63±0.04	15.24±0.07	CFHT
CFHT-Pl 25	16.68±0.02	15.87±0.04	15.48±0.07	CFHT
Roque 16	15.52±0.02	14.87±0.04	14.50±0.07	CFHT
	15.67±0.03		14.56±0.10	MHO

Note. — The error bars are 1 σ standard deviations.

Table 3. Spectroscopic log

Name	Date	Telescope	Grating	Disp. (Å/pix)	Range (nm)	$\tau_{\rm exp}$ (s)
CFHT-Pl 1	1998 Dec 22	KPNO	730	4.20	533.9–959.7	900
CFHT-Pl 2	1998 Dec 22	KPNO	730	4.20	533.9–959.7	900
CFHT-Pl 5	1998 Dec 23	KPNO	730	4.20	533.9–959.7	900
CFHT-Pl 6	1998 Dec 23	KPNO	730	4.20	533.9–959.7	900
CFHT-Pl 7	1998 Dec 22	KPNO	730	4.20	533.9–959.7	1800
CFHT-Pl 8	1998 Dec 22	KPNO	730	4.20	533.9–959.7	1200
CFHT-Pl 16	1998 Dec 22	KPNO	730	4.20	533.9–959.7	1800
CFHT-Pl 16	2000 Jan 5	Keck II	900	0.85	631.2–802.9	3600
CFHT-Pl 17	1998 Dec 22	KPNO	730	4.20	533.9–959.7	1800
CFHT-Pl 18	1998 Dec 21	Keck II	900	0.85	631.2–802.9	5400
CFHT-Pl 19	1998 Dec 22	KPNO	730	4.20	533.9–959.7	1800
CFHT-Pl 20	1998 Dec 23	KPNO	730	4.20	533.9–959.7	1800
CFHT-Pl 25	1998 Dec 23	Keck II	150	4.82	355.5–1125.1	1200
CFHT-Pl 26	1998 Dec 23	Keck II	150	4.82	355.5–1125.1	1800
Roque 7	1997 Dec 28	WHT	158	2.91	629.1–926.5	2000
Roque 25	1998 Dec 23	Keck II	150	4.82	355.5–1125.1	1800
Roque 33	1998 Dec 23	Keck II	150	4.82	355.5–1125.1	2000
Teide 1	1998 Dec 23	Keck II	150	4.82	355.5–1125.1	1200

Table 4. Spectroscopic data

Name	PC3	SpT	TiO	VO	H_α
					(Å)
CFHT-Pl 1	1.26	dM4.9	2.56	2.41	-3.1±0.5
CFHT-Pl 2	1.26	dM4.9	3.09	2.43	-3.4±0.5
CFHT-Pl 5	1.36	dM5.5	3.26	2.52	-4.0±0.5
CFHT-Pl 6	1.61	dM6.9	3.52	2.70	≥-2
CFHT-Pl 7	1.37	dM5.6	3.08	2.43	≥-2
CFHT-Pl 8	1.37	dM5.6	3.09	2.51	-14.6±0.4
CFHT-Pl 16	2.20	dM9.3	4.41	2.74	≥-15
CFHT-Pl 16*					-6.1±0.3
CFHT-Pl 17	1.82	dM7.9	4.48	2.86	-7:
CFHT-Pl 18*					-3.0±0.2
CFHT-Pl 19	1.68	dM7.5	4.07	2.50	≥-10
CFHT-Pl 20	1.71	dM7.5	3.55	2.51	≥-3
CFHT-Pl 25	2.10	dM9.0	4.75	3.06	≥-6
CFHT-Pl 26	1.65	dM7.1	3.76	3.20	≥-5
Roque 7	1.90	dM8.3	4.60	2.89	≥-15
Roque 25	2.58	dL0.1	2.61	2.51	-9±2
Roque 33	2.44	dM9.8	6.35	3.20	-55±10
Teide 1	1.81	dM7.9	4.22	2.80	-2:

*Measurement using intermediate resolution spectrum

Note. — A colon indicates uncertain detection due to low S/N ratio or blending.

Table 5. Limits to the presence of companions in the NIC1 frames

Name	Δ m(F110M)	Δ m(F165M)	Δ m(F110M)	Δ m(F165M)
	(0”.1)	(0”.1)	(0”.4)	(0”.4)
Calar 3			1.0	1.0
CFHT-Pl 15*	2.6	3.4	5.2	4.5
CFHT-Pl 16	4.3	4.5	4.8	5.0
CFHT-Pl 17	4.0	4.6	4.9	5.6
CFHT-Pl 19*	2.1	3.7	4.6	4.4
CFHT-Pl 22	3.5	4.0	4.2	4.2
CFHT-Pl 23	3.9	4.1	4.7	5.2
CFHT-Pl 25	4.2	5.1	5.2	5.5
HHJ 2*	3.3	4.5	5.6	5.5
HHJ 8	3.0	3.0	4.5	4.5
MHO 1	3.7	4.7	5.0	5.3
MHO 3*	2.9	3.8	5.1	5.5
MHO 6	3.0	3.0	4.5	4.5
PIZ 1	3.1	4.1	3.5	4.4
PPl 1	4.6	4.8	5.8	5.8
PPl 14	4.6	4.7	5.2	5.4
Roque 4	4.2	4.4	4.7	5.2
Roque 7	3.9	4.1	4.7	5.5
Roque 11	3.0	3.0	4.5	4.5
Roque 12	3.0	3.0	4.5	4.5
Roque 13	4.2	4.6	5.4	5.5
Roque 14	4.1	4.5	5.3	5.7
Roque 16	4.6	4.4	5.7	5.6
Roque 17	3.9	4.2	5.5	5.2

Table 5—Continued

Name	Δ m(F110M)	Δ m(F165M)	Δ m(F110M)	Δ m(F165M)
Roque 25	3.0	3.8	3.3	3.9
Teide 1	4.1	4.1	5.4	4.9
Teide 2	4.0	4.3	4.7	5.2

[*] Residuals in the PSF subtraction, possibly due to the presence of an unresolved companion with brightness close to the Δm limit given in this Table and separation less than 0".22

Table 6. Membership status

Name	Dwarf?	V_{rad}	pm	Li	H_α	SpT	I-K	NIC	Member?
Calar 3	Yes	Yes		Yes	Yes	Yes	Yes		Yes
CFHT-Pl 1	Yes				Yes	Yes	Yes		Yes
CFHT-Pl 2	Yes				Yes	Yes	Yes		Yes
CFHT-Pl 3*	Yes		Yes				Yes		Yes
CFHT-Pl 4							Yes		Yes?
CFHT-Pl 5	Yes				Yes	Yes	Yes		Yes
CFHT-Pl 6	Yes				No	Yes	Yes		Yes?
CFHT-Pl 7	Yes				No	Yes	Yes		Yes?
CFHT-Pl 8	Yes				Yes	Yes	Yes		Yes
CFHT-Pl 9	Yes			No	Yes		Yes		Yes
CFHT-Pl 10	Yes			No	Yes		Yes		Yes
CFHT-Pl 12	Yes			Yes	Yes		Yes	Yes	Yes
CFHT-Pl 14	Yes		No	No	No				No
CFHT-Pl 15	Yes			Yes	Yes		Yes	Yes	Yes
CFHT-Pl 16	Yes	Yes		Yes	Yes	Yes	Yes	Yes	Yes
CFHT-Pl 17	Yes				Yes	Yes	Yes	Yes	Yes
CFHT-Pl 18	Yes			No	Yes	Yes	Yes	No	No
CFHT-Pl 19	Yes					Yes	No	Yes	No?
CFHT-Pl 20	Yes				No	Yes	No	No	No
CFHT-Pl 22	Yes					Yes	No	No	No
CFHT-Pl 23	Yes						Yes	Yes	Yes
CFHT-Pl 25	Yes				No	Yes	Yes	Yes	Yes
CFHT-Pl 26	Yes				No	No			No
HHJ 2	Yes		Yes		Yes	Yes	Yes	Yes	Yes
HHJ 6	Yes	Yes	Yes		Yes	Yes	Yes	Yes	Yes

Table 6—Continued

Name	Dwarf?	V_{rad}	pm	Li	H_α	SpT	I-K	NIC	Member?
HHJ 8	Yes		Yes		Yes	Yes	Yes	Yes	Yes
MHO 1								No	No
MHO 3	Yes	Yes		Yes	Yes			Yes	Yes
MHO 6								Yes	Yes?
PIZ 1	Yes					Yes	Yes	Yes	Yes
PPl 1	Yes	Yes		Yes	Yes	Yes	Yes	Yes	Yes
PPl 14	Yes				Yes	Yes		No	No?
PPl 15	Yes	Yes	Yes	Yes	Yes	Yes	Yes		Yes
Roque 4	Yes	Yes			Yes	Yes	Yes	Yes	Yes
Roque 7	Yes					Yes		Yes	Yes
Roque 11	Yes	Yes			Yes	Yes	Yes	Yes	Yes
Roque 12	Yes				Yes	Yes	Yes	Yes	Yes
Roque 13	Yes			Yes	Yes		Yes	Yes	Yes
Roque 14	Yes			Yes	Yes	Yes		Yes	Yes
Roque 16	Yes			Yes	Yes		Yes	Yes	Yes
Roque 17	Yes			Yes	Yes	Yes		Yes	Yes
Roque 25	Yes				Yes	Yes	Yes	Yes	Yes
Roque 33	Yes			Yes	Yes	Yes			Yes
Teide 1	Yes	Yes	Yes	Yes	Yes	Yes	Yes	Yes	Yes
Teide 2	Yes	Yes		Yes	Yes	Yes	Yes	Yes	Yes

[*] Dwarf status inferred from proper motion because a spectrum is not available.

Table 7. Binary frequency

$N_{objects}$	$N_{binaries}$	$N_{expected}$	Sep. range (")	Dist. range (AU)	q_{min}	log P (d)
24	2*	0.6	<0.08	<10.9	0.8	<4.60
34	4*	3.0	<0.2	<27.2	0.6	<5.21
34	0	1.8	0.2-1.0	27.2-135.9	0.4	5.21-6.26
44	0	1.6	1.0-8.0	135.9-1087.0	0.5	6.26-7.62

[*] Only one binary confirmed spectroscopically (PPl 15). CFHT-Pl-12, CFHT-Pl-16, and HHJ 6 are inferred to be binaries with nearly identical components because of their position in Figure 2, but they are not resolved with HST or AO images. q_{min} is the average minimum mass ratio (M_2/M_1) for a binary to be detected with our data.

Figure Captions:

Fig. 1.— A NICMOS color-magnitude diagram. Lithium-confirmed Pleiades members are plotted with red color. The location of some important objects are indicated. PPl 1 has two positions in the plot because it is variable. We have used a Pleiades distance of 125 pc for calculating absolute magnitudes. The solid line (blue) is the 120 Myr isochrone for dust-free Nextgen model atmospheres. The dashed line (magenta) is an isochrone for the same age but Dusty model atmosphere. The cyan horizontal line joins the points corresponding to a mass of 0.04 $M_\odot$ for Nextgen and Dusty models.

Fig. 2.— A color-magnitude diagram with the ground-based near-IR photometry. Lithium confirmed BDs are denoted with filled pentagons. Objects that follow the cluster sequence are represented with emply pentagons. Objects that lie well below the sequence (likely non-members) are plotted as five pointed stars. The solid lines are the 100 Myr and 120 Myr isochrones for NextGen model atmospheres. The dashed lines are Dusty isochrones for the same ages. Dotted lines join points of the same mass (labelled in solar units) in different isochrones.

Fig. 3.— Keck LRIS low-resolution spectra of the coolest objects in our sample.

Fig. 4.— Spectral Types of Pleiades BD candidates versus observed I-band magnitudes. Filled symbols represent objects with lithium detections.

Fig. 5.— Keck LRIS mid-resolution spectra of CFHT-Pl-16 and 18. The spectrum of Teide 1 (Rebolo et al. 1996) is also shown for comparison. We have applied a boxcar smoothing of 3 pixels to all the spectra. H_α is seen in emission, and the LiI resonance line at 670.8 nm is detected in CFHT-Pl-16 but not in CFHT-Pl-18.

Fig. 6.— Reduced HST/NIC1 images of CFHT-Pl 17 before and after PSF subtraction. The

name of the object used for the subtraction is given on the right-hand side.

Fig. 7.— Examples of radially averaged sensitivity limits to the presence of companions after PSF subtraction.

Fig. 8.— Mass-Luminosity relationships in different NIR filters given by Nextgen (solid line) and Dusty (dotted line) models for an age of 120 Myr.

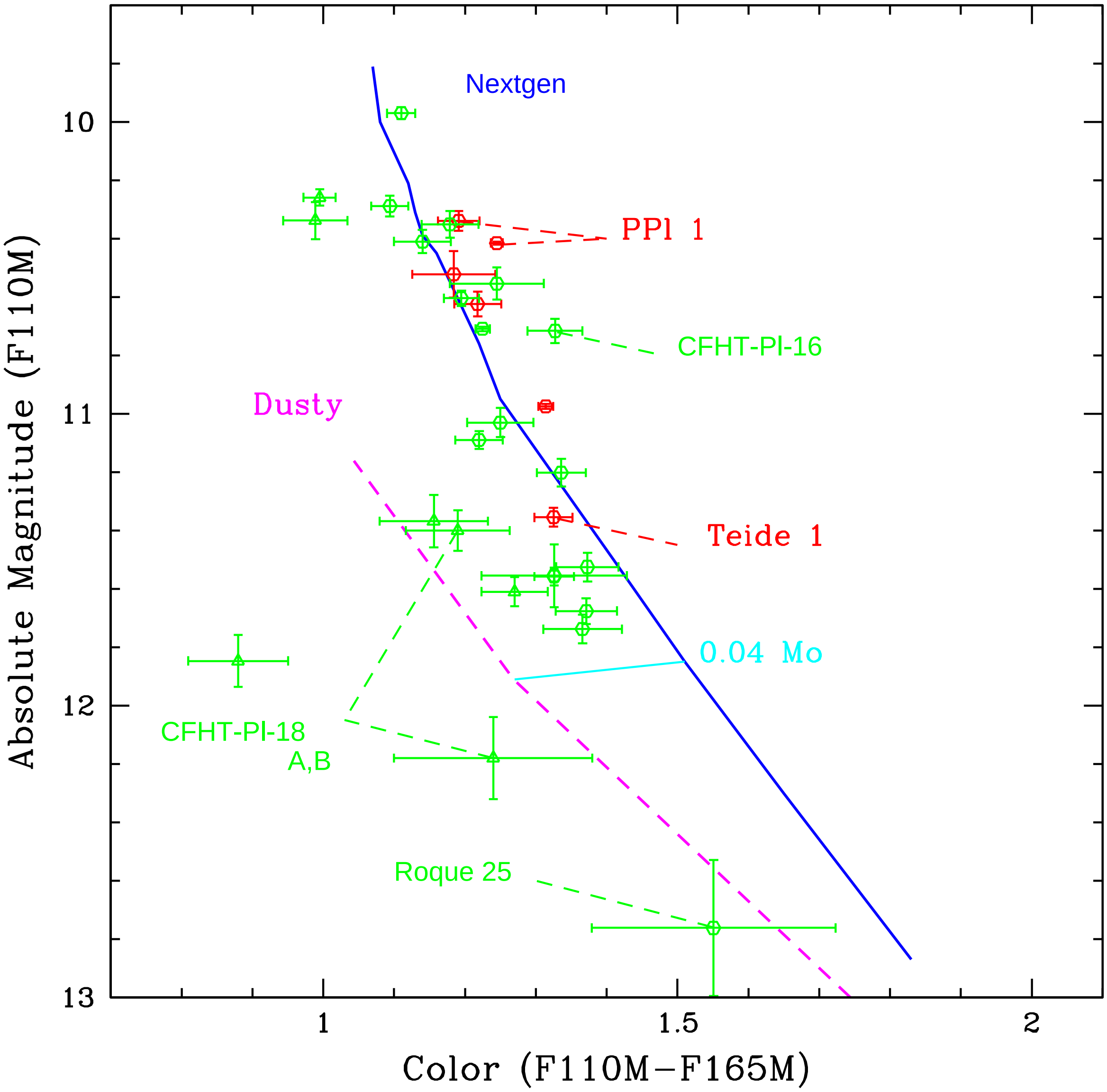
Nextgen
PPl 1
CFHT-Pl-16
Dusty
Teide 1
0.04 Mo
CFHT-Pl-18
A,B
Roque 25
10
11
12
13
1
1.5
2
Absolute Magnitude (F110M)
Color (F110M−F165M)

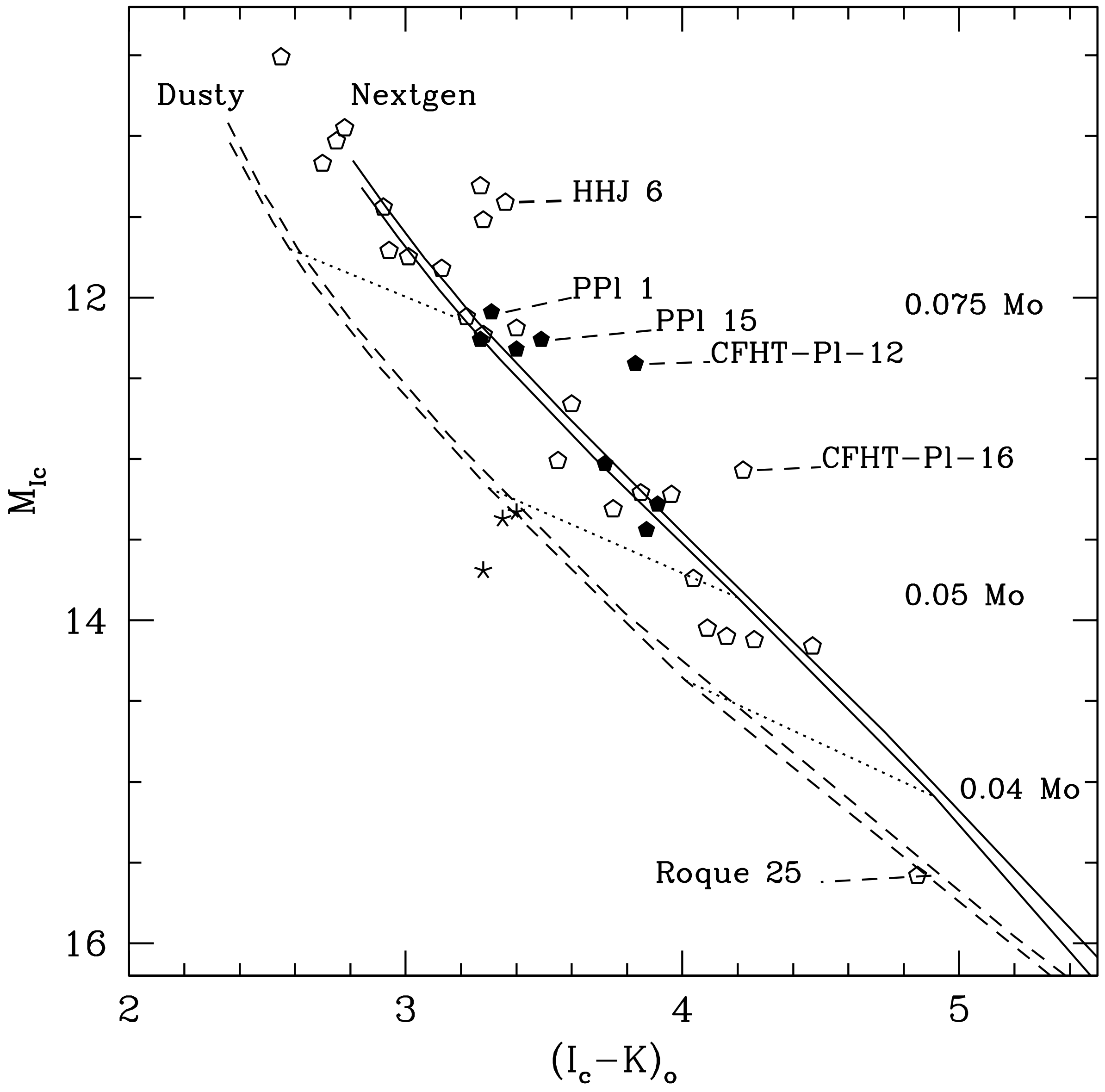
Dusty
Nextgen
HHJ 6
PPl 1
PPl 15
CFHT–Pl–12
CFHT–Pl–16
0.075 Mo
0.05 Mo
0.04 Mo
Roque 25
12
14
16
2
3
4
5
M_{Ic}
$(I_c-K)_o$

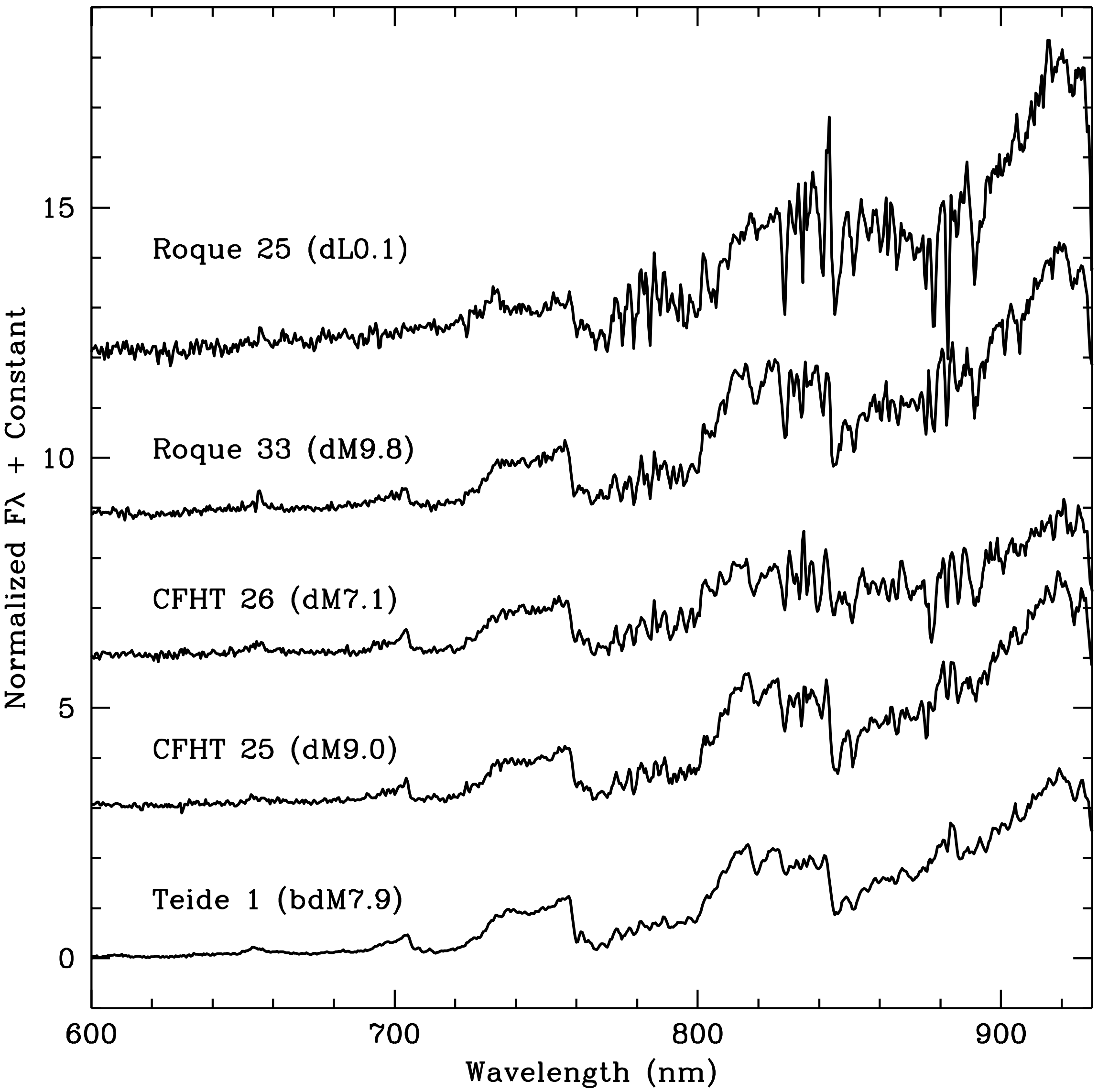
Roque 25 (dL0.1)
Roque 33 (dM9.8)
CFHT 26 (dM7.1)
CFHT 25 (dM9.0)
Teide 1 (bdM7.9)
Normalized Fλ + Constant
0
5
10
15
600
700
800
900
Wavelength (nm)

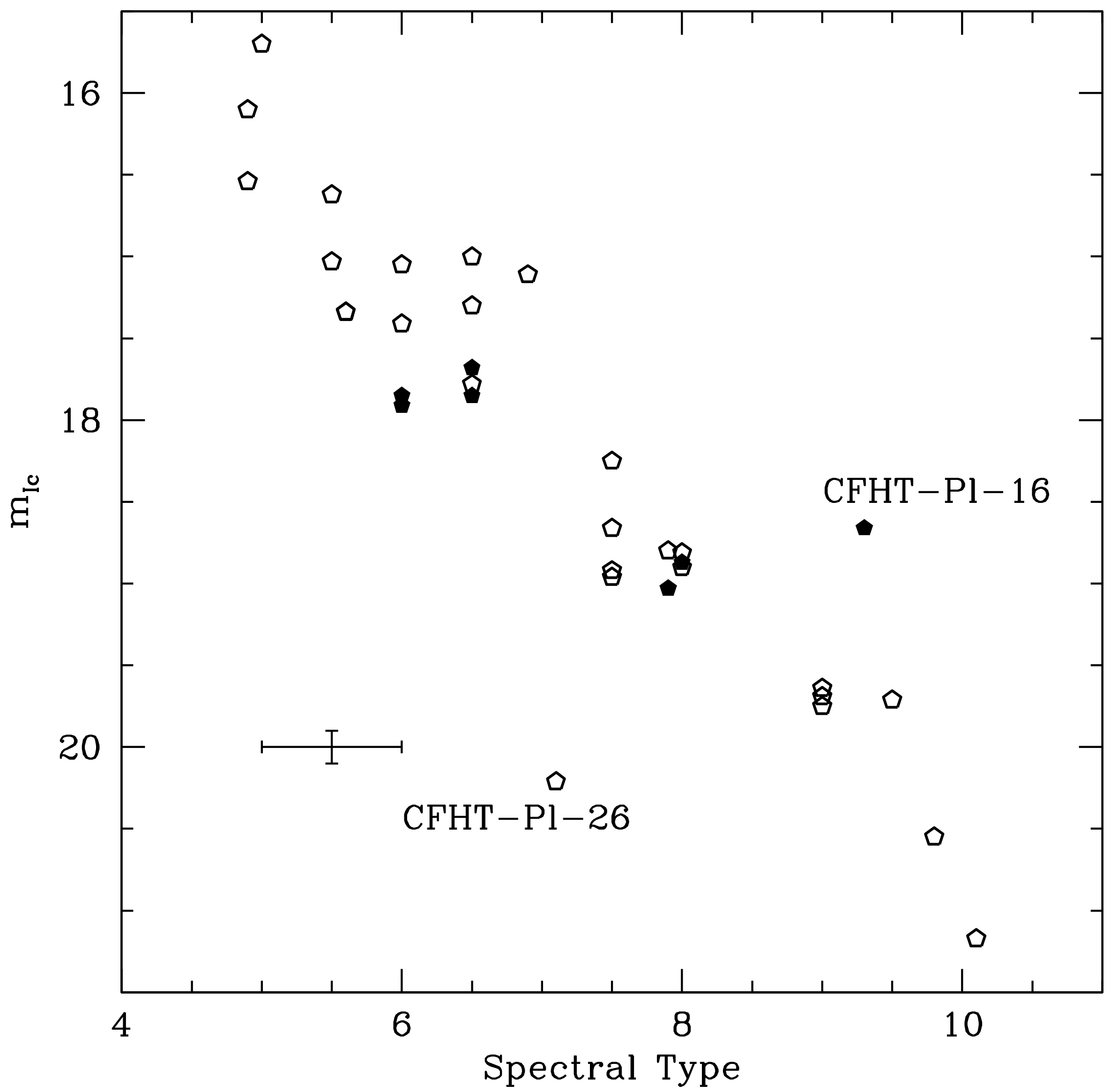
16
18
20
4
6
8
10
m_{Ic}
Spectral Type
CFHT−Pl−16
CFHT−Pl−26

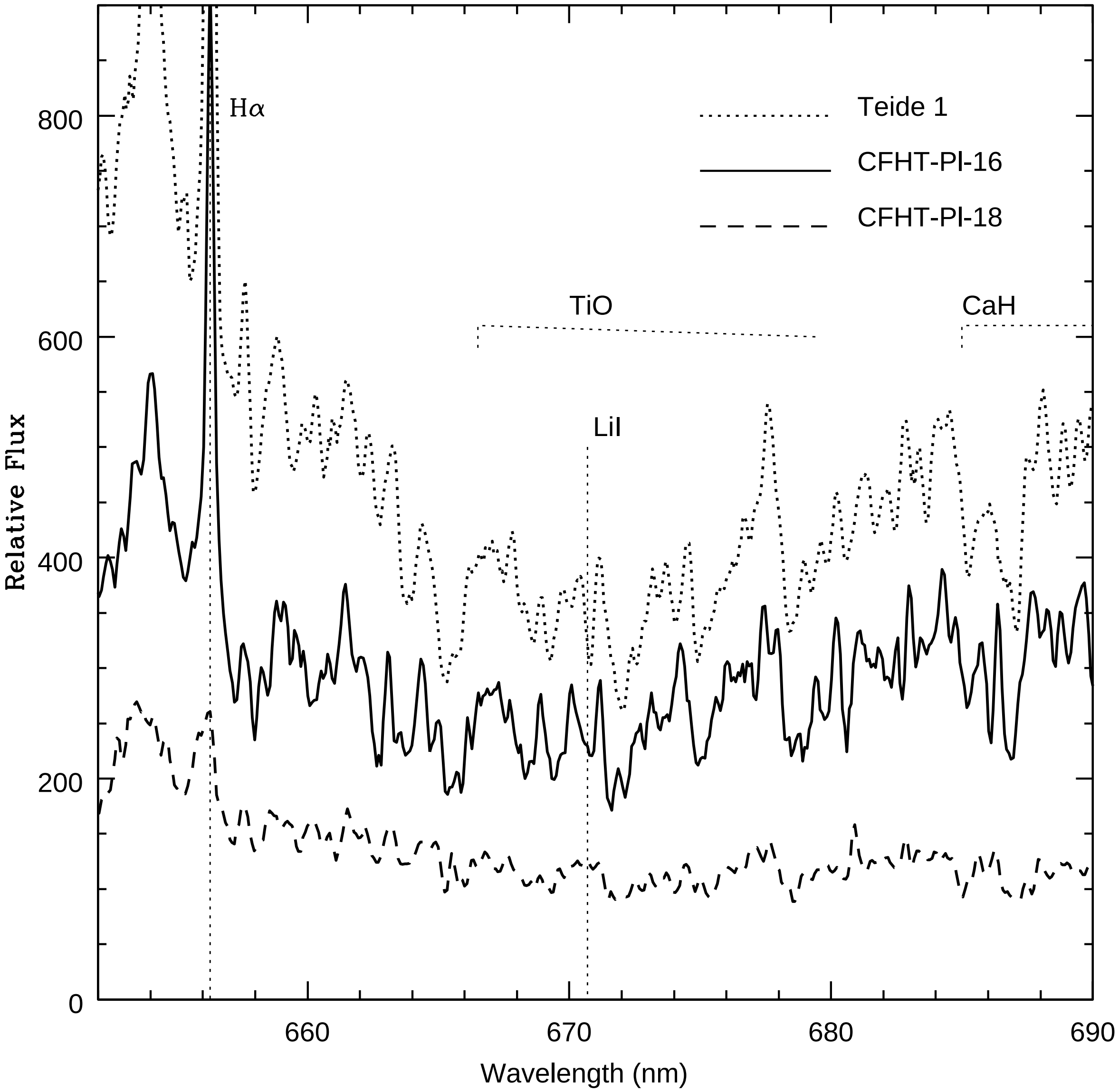
Relative Flux
0
200
400
600
800
660
670
680
690
Wavelength (nm)
Hα
TiO
CaH
LiI
Teide 1
CFHT-Pl-16
CFHT-Pl-18

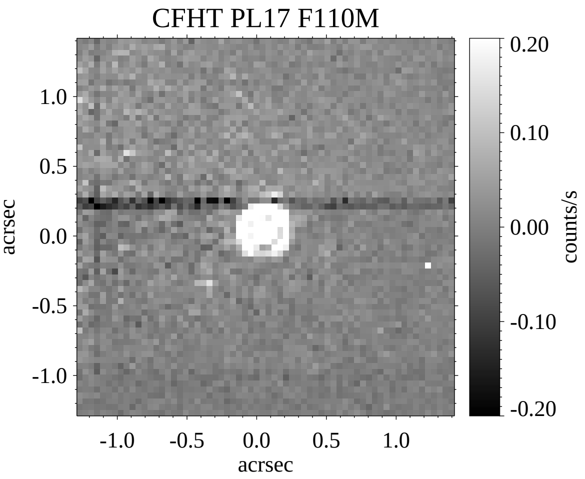
CFHT PL17 F110M
acrsec
acrsec
counts/s
0.20
0.10
0.00
-0.10
-0.20
1.0
0.5
0.0
-0.5
-1.0

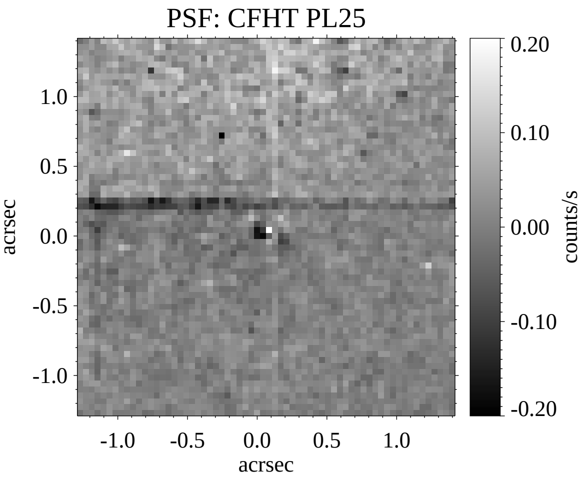
PSF: CFHT PL25
acrsec
acrsec
counts/s
0.20
0.10
0.00
-0.10
-0.20
1.0
0.5
0.0
-0.5
-1.0

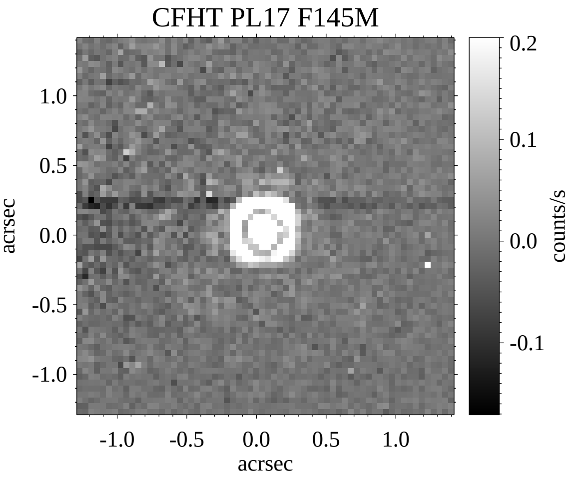
CFHT PL17 F145M
acrsec
acrsec
counts/s
0.2
0.1
0.0
-0.1
1.0
0.5
0.0
-0.5
-1.0

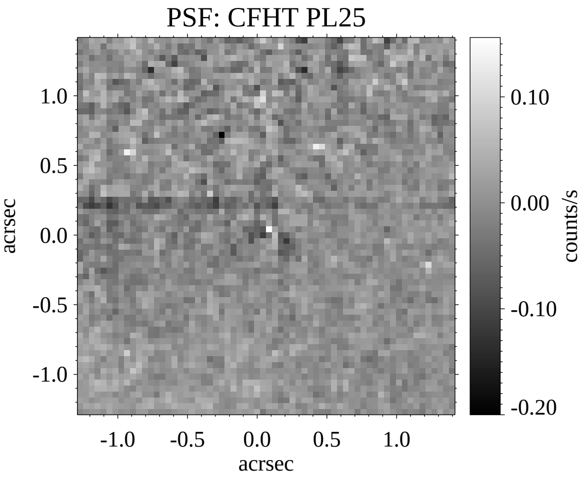
PSF: CFHT PL25
acrsec
acrsec
counts/s
0.10
0.00
-0.10
-0.20
1.0
0.5
0.0
-0.5
-1.0

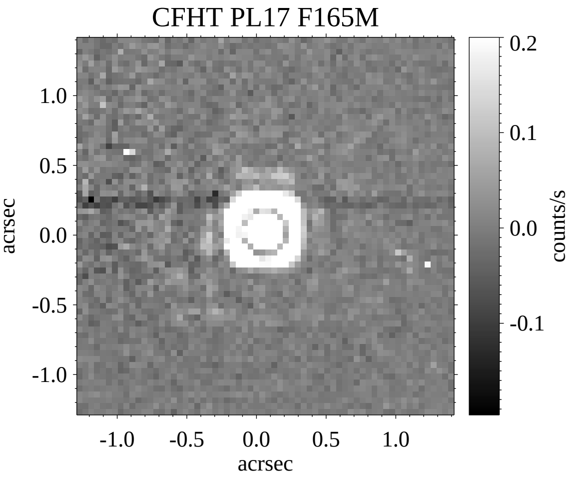
CFHT PL17 F165M
acrsec
acrsec
counts/s
0.2
0.1
0.0
-0.1
1.0
0.5
0.0
-0.5
-1.0

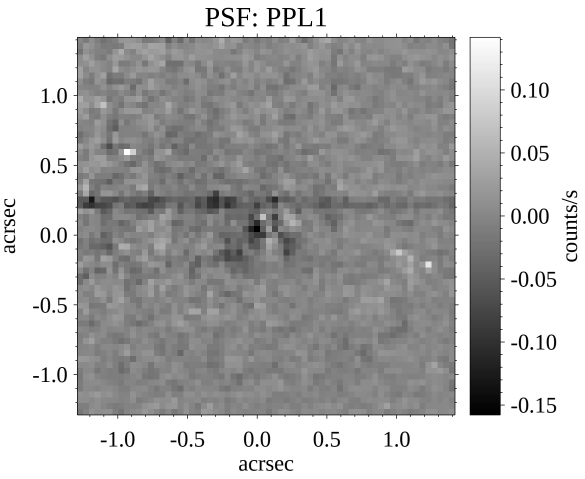
PSF: PPL1
acrsec
acrsec
counts/s
0.10
0.05
0.00
-0.05
-0.10
-0.15
1.0
0.5
0.0
-0.5
-1.0

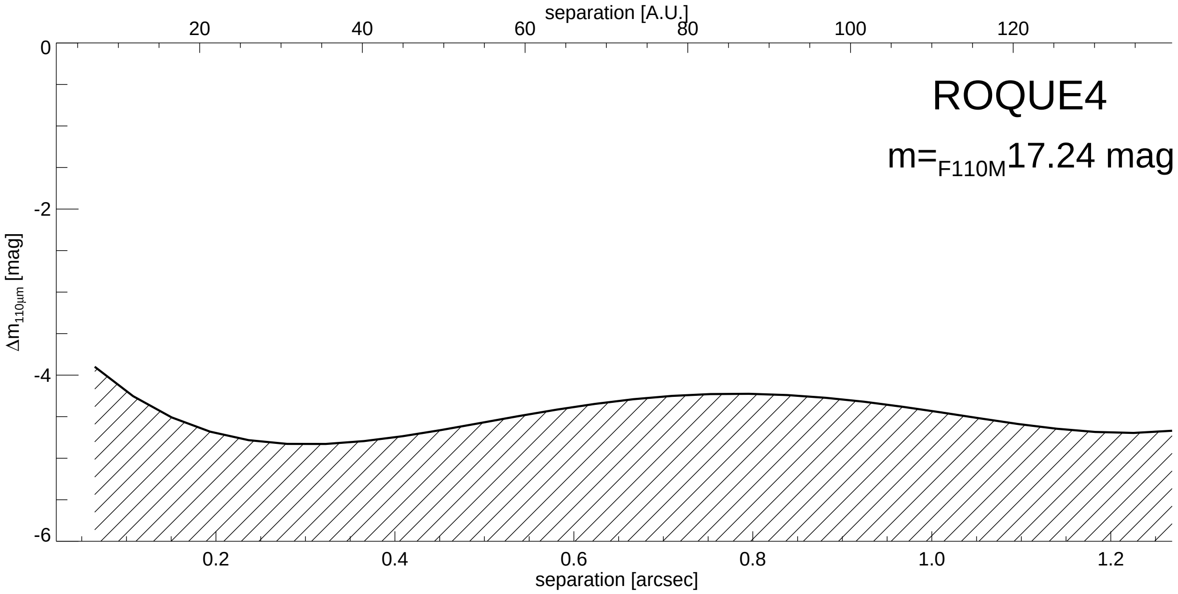
separation [A.U.]
20
40
60
80
100
120
0
-2
-4
-6
Δm110µm [mag]
ROQUE4
m=F110M17.24 mag
0.2
0.4
0.6
0.8
1.0
1.2
separation [arcsec]

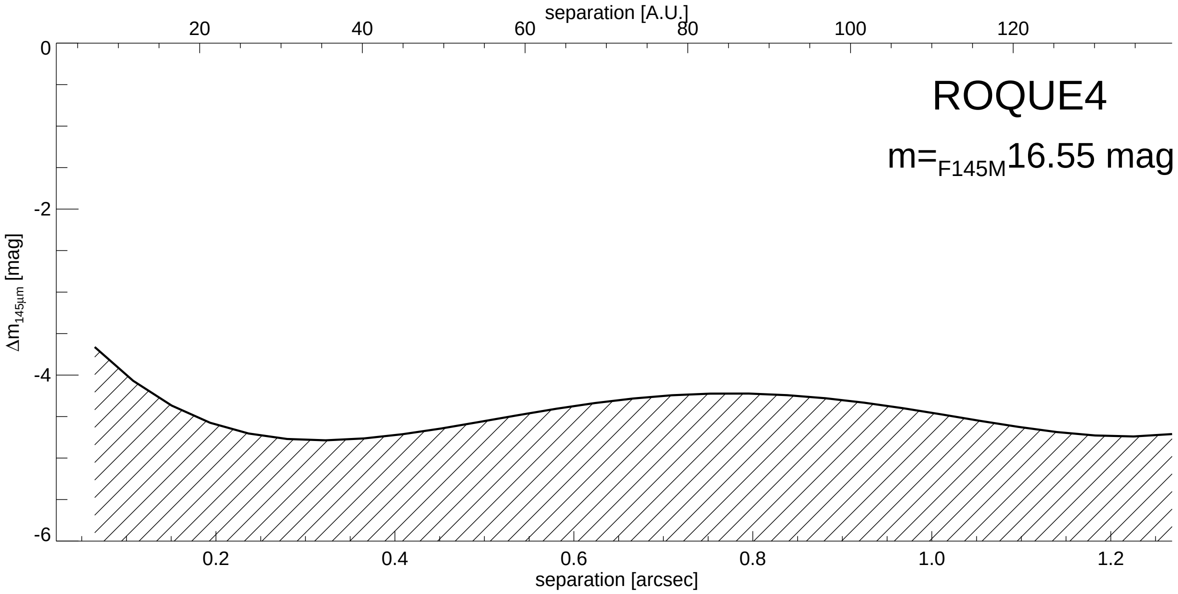
separation [A.U.]
20
40
60
80
100
120
0
-2
-4
-6
Δm145µm [mag]
ROQUE4
m=F145M16.55 mag
0.2
0.4
0.6
0.8
1.0
1.2
separation [arcsec]

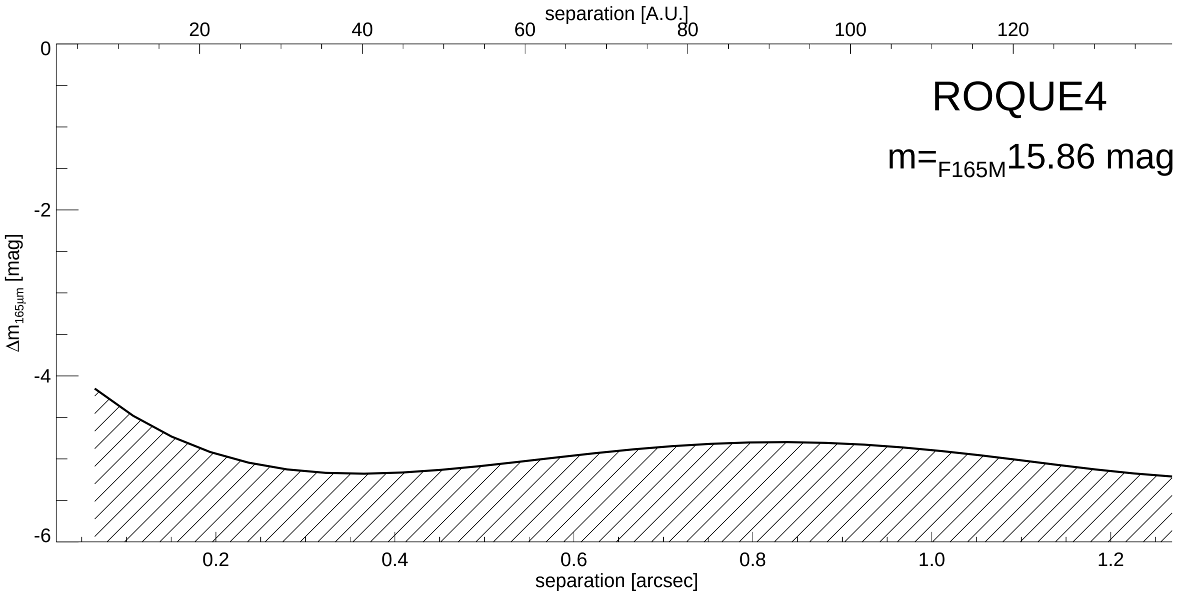
separation [A.U.]
20
40
60
80
100
120
0
-2
-4
-6
Δm165µm [mag]
ROQUE4
m=F165M15.86 mag
0.2
0.4
0.6
0.8
1.0
1.2
separation [arcsec]

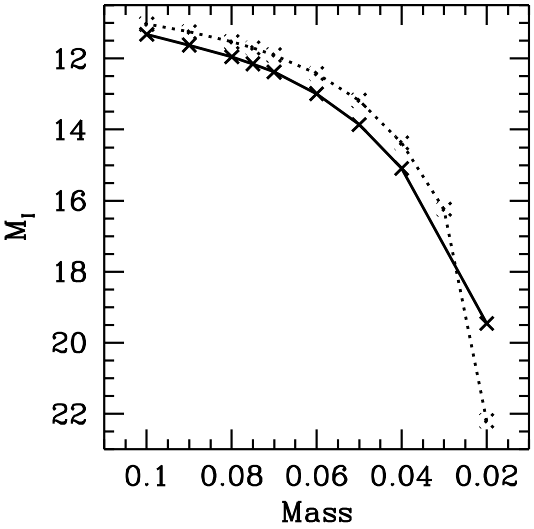
M_I
12
14
16
18
20
22
0.1
0.08
0.06
0.04
0.02
Mass

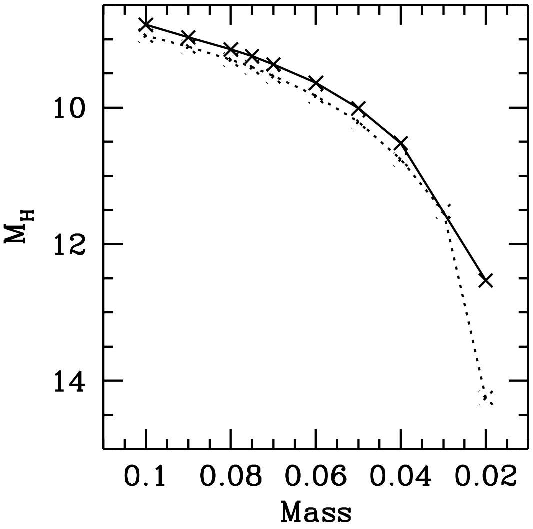
M_H
10
12
14
0.1
0.08
0.06
0.04
0.02
Mass

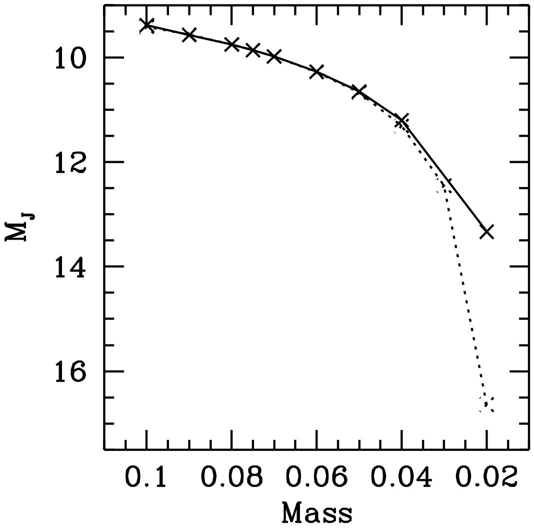
M_J
10
12
14
16
0.1
0.08
0.06
0.04
0.02
Mass

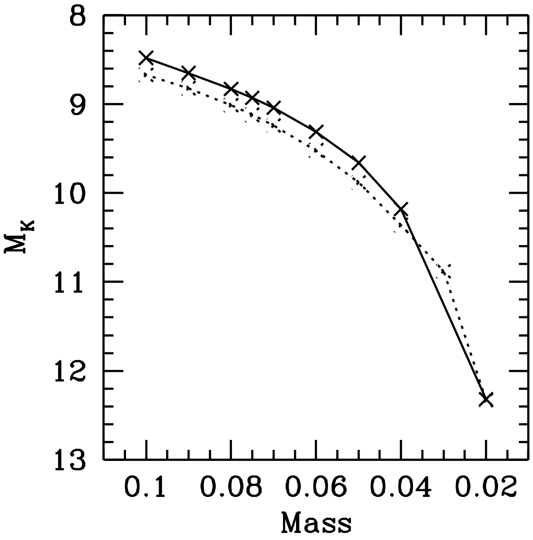
M_K
8
9
10
11
12
13
0.1
0.08
0.06
0.04
0.02
Mass